Article

Enhancement of CO$_2$ Removal Efficacy of Fluidized Bed Using Particle Mixing

Ebrahim H. Al-Ghurabi, Abdelhamid Ajbar and Mohammad Asif *

Department of Chemical Engineering, King Saud University, PO Box 800, Riyadh 11421, Saudi Arabia; alghurabi83@windowslive.com (E.H.A.-G.); aajbar@ksu.edu.sa (A.A.)

* Correspondence: masif@ksu.edu.sa; Tel.: +966-56-981-7045

check for updates

Featured Application: Towards developing a cost-effective technique based on the fluidized bed technology for the treatment of carbon dioxide in flue gases. We have clearly shown that assisted fluidization technique of particle mixing proposed here can improve the CO$_2$ capture efficacy of fluidized bed containing fine adsorbent.

Abstract: The present study proposes a cost-effective assisted fluidization technique of particle mixing to improve the carbon capture effectiveness of a fluidized bed containing fine adsorbent powder. Using activated carbon as the adsorbent, we mixed external particle of Geldart group B classification in different fractions to examine the effectiveness of the proposed strategy of particle mixing. Four different particle-mixing cases were considered by varying the amount of added particle—0, 5, 10, and 30 wt %—on external particle-free basis. The inlet flow of the nitrogen was fixed, while two different flows of carbon dioxide were used. The adsorption experiment consisted of a three step procedure comprising purging using pure nitrogen, followed by adsorption with fixed inlet CO$_2$ concentration, and finally the desorption step. Inlet flows of both nitrogen and CO$_2$ were separately controlled using electronic mass flow controllers with the help of data acquisition system (DAQ). The CO$_2$ breakthrough was carefully monitored using the CO$_2$/O$_2$ analyzer, whose analog output was recorded using the DAQ. Best results were obtained with 10% external particles. This is in conformity with the results of our previous study of bed hydrodynamics, which pointed to clear improvement in the fluidization behavior with particle mixing.

1. Introduction

Although carbon dioxide (CO$_2$) constitutes only 0.035% of the atmosphere, it is one of the most abundant greenhouse gases (GHG). The widespread use of fossil fuel combustion in energy-intensive industrial activities accounts for 90% of total CO$_2$ emissions [1,2]. The transition from carbon-based energy sources to cleaner ones would be an ideal solution; however, the proposed technologies are still not mature enough to allow for their large-scale implementation. Therefore, technologies for carbon capture and sequestration (CCS) will continue to play an important role until significant changes in the energy infrastructure can be achieved.

The CO$_2$ capture process constitutes the major component of the total CCS cost [3,4]. Research efforts have therefore focused on developing new techniques to reduce the economic cost while achieving significant levels of CO$_2$ capture. Several technologies are available for this purpose. These include absorption, membrane separation, biofixation, and adsorption [5–7]. Commonly used in the chemical process industries, the use of absorption using solvents has also

been applied to postcombustion flue gases, e.g., Boundary Dam power station in Saskatchewan, Canada [8]. This technology, however, requires expensive pretreatment of the flue gases and is moreover energy-intensive. In addition, the solvent evaporation and equipment corrosion are two other important issues that also require careful consideration for the long-term viability of this technology. The use of the membrane separation technology has recently attracted considerable interest. However, some recent studies have suggested that this technology does not offer any notable advantage over chemical absorption, in terms of both energy consumption and cost [9], unless fresh approach towards the development of novel types of membranes are adopted. For example, mixed-matrix membranes (MMMs) composed of a polymer and activated carbon showed good performance in the separation of gases [10,11]. Another environment-friendly approach proposed in the recent literature is microbial CO_2 biosequestration using microorganisms [12]. However, its application still requires considerable further basic research and applied development work. Among these technologies, adsorption is attractive in the long term owing to its operational flexibility, low energy requirements, and generally low maintenance costs [4,13–16]. Adsorption consists of an uptake of CO_2 molecules onto the solid surface, which can occur via either weak van der Waals forces (physisorption) or stronger covalent bonding (chemisorption) [15]. However, adsorption also has potential disadvantages, including handling large volumes of adsorbent, particles attrition, and thermal control of large-scale adsorber vessels. The efficiency of adsorption depends naturally on the adsorbents used. In this regard, there are a number of efficient solid adsorbents for CO_2 that include activated carbons, activated alumina, zeolites, ion-exchange resins, silica gel, metal oxides, mesoporous silicates, carbon fibers and their composites, and metal-organic frameworks (MOF) [17]. For the adsorption to become economically viable, the selection of a suitable adsorbent material is important. An ideal CO_2 adsorbent should have high adsorption capacity, high hydrophobicity and tolerance to feed impurities, stability, low cost, and ease of regeneration [17]. Activated carbon powders, when used as adsorbents, possess a number of such characteristics. For example, they are insensitive to moisture, have low cost, and require low energy for regeneration [18] despite having relatively lower adsorption capacity [19].

For gas–solid contacting during the adsorption, either fixed bed or fluidized bed mode can be implemented. The application of fluidized bed instead of fixed bed yields lower pressure drop, better phase contact, and intimate mixing that ultimately translates into greater efficiency and lower costs [20,21]. Moreover, fluidization is particularly suitable compared to other available techniques for handling and processing large quantities of powders. While fine powders can theoretically provide a high surface area for the adsorption, the efficacy of gas–solid contact during fluidization is often severely compromised by the agglomeration of the fine particles as a result of interparticle van der Waals forces. For example, the fluidization of fine cohesive powders of Geldart group C is rather heterogeneous and is characterized by the formation of cracks and channels through which the gas phase tends to bypass solids present in the bed, resulting in poor contact and inefficient mixing [12–24]. This phenomenon can significantly lower the CO_2 adsorption capacity of the fine adsorbent.

In order to improve the fluidization hydrodynamics of solids that exhibit poor fluidization behavior, various assisted fluidization techniques have been proposed in the literature [24–34]. These techniques are generally implemented in conjunction with conventional fluidization to provide additional energy to the fluidized bed for overcoming interparticle forces that cause powder cohesiveness and other nonhomogeneities observed during fluidization. A recent interesting example of such assisted fluidization techniques is the continuous pulsation of inlet flow at regular time intervals instead of a continuous steady inlet flow of the gas to the fluidized bed. This technique greatly improves the fluidization hydrodynamics of ultrafine powders [26,27,35–38]. Similarly, the use of acoustic vibrations has also been reported in the literature [28–30,39–41]. These vibrations promote deagglomeration and eliminate bed nonhomogeneities, thus improving the gas–liquid phase contact. The CO_2 removal efficacy of sound-assisted fluidized bed significantly improves as a result of acoustic

perturbations [41–45]. However, although effective, this technique is inherently energy intensive and moreover requires modification in the fluidization setup for the installation of sound system.

Another simple yet cost-effective assisted fluidization technique is the addition of external inert particles. A carefully chosen sample of external particles with appropriate physical properties, when mixed with resident solid phase of the fluidized bed, has been found to significantly enhance fluidization hydrodynamics [23,30,31,46]. For example, the addition of Group A particles to a bed of nanopowder was found to promote deagglomeration and suppress the phenomenon of hysteresis [31,46]. In the present work, we applied this technique to improve the CO_2 capture efficacy of a fluidized bed containing fine adsorbent particles. This was achieved by adding inert external particles of Geldart group B classification. This choice was dictated by the encouraging results of a recent study that clearly demonstrated the effectiveness of the particle-mixing strategy utilizing Group B particles in improving the hydrodynamics of the fluidized bed of Group C particles [47]. Two different Group C particles—activated carbon and calcium hydroxide—were considered, while the fraction of external particle used for mixing was varied. The bed hydrodynamics was characterized using the fluidization index. A statistical evaluation of results clearly indicated that the best fluidization is achieved when the proportion of inert particle is 10–15 wt % on the external particle free basis. We therefore extended the same strategy of particle mixing to improve the CO_2 removal efficacy of fluidized bed containing fine adsorbent particles. Needless to mention, the basic fluidization setup remains unchanged for the implementation of the proposed particle-mixing strategy; moreover, there was no extra consumption of energy besides the one associated with the pressure drop. The use of inert sand as the external group B particles further minimized the cost component of the proposed strategy.

2. Experimental

Experimental Setup

Figure 1 shows the schematic diagram of the experimental setup. The test section comprised a 1-m-long vertical Perspex column of 70-mm internal diameter. A perforated plate distributor, located at its bottom, ensured a uniform distribution of inlet gases. The distributor was a 10-mm-thick Plexiglas plate with 1.5-mm holes and 4% open area. To eliminate entry effects, a 250-mm-long calming section was provided below the distributor, as shown in the figure. The outlet gases from the column were released outside the lab to prevent nitrogen and CO_2 build-up. Openings along the column height provided ports for the measurement of the pressure drop and the carbon dioxide concentration. Before the start of the experiment, the setup was tested for any leaks by ensuring inlet and outlet flows were equal.
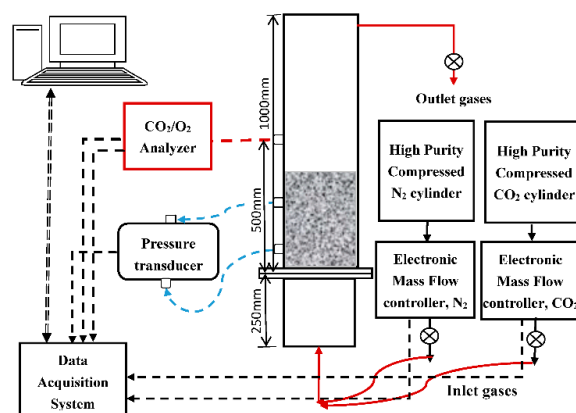

Figure 1. Schematic of the experimental setup for the CO_2 adsorption from the mixture of N_2–CO_2 gases. Single black broken lines represent voltage signal connections of different equipment with data acquisition system (DAQ); double black broken lines represent communication of DAQ with computer.

As shown in Figure 1, the inlet gas flow assembly comprised two separate inlet lines from compressed cylinders of nitrogen and carbon dioxide. To ensure accurate measurement of the flow rates of gases, two different electronic flow controllers of different ranges were used. For nitrogen, the range was 0–2 SLPM (FMA-2605A-V2P), while 0–200 CCPM (FMA-2618A-V2P) was used for the carbon dioxide. Excellent linearity between the voltage output and the flow rate was noticed. The analog voltage inputs and outputs of the mass flow controllers were connected to the data acquisition system (DAQ) for controlling and monitoring the flow of gases to the column. Both gases were mixed in fixed proportion before entering the test section of the fluidized bed.

For the measurement of the carbon dioxide concentration, we used an oxygen/carbon dioxide analyzer (Model 902P, Quantek Instruments, Grafton, MA, USA) in view of its high accuracy and measurement stability. The analog output options for the carbon dioxide and the oxygen were configured and connected to the data acquisition system. The minimum CO_2 detection limit was 0.01%, while the upper concentration range was 20%. National Institute of Standards and Technology (NIST) traceable calibration certificate, supplied by the manufacturer, was used for converting the voltage output to percentage volumetric concentration. The voltage signals from the analyzer were captured by DAQ running LabView software and then transferred to a computer for further processing.

We employed a fast response pressure transducer for monitoring the local transients of the fluidized bed. It was a sensitive, differential, bidirectional pressure transducer (PX163-005BD5V, Omega, Stamford, CT, USA) with a response time of 1 millisecond. As shown in Figure 1, the lower pressure port was located at a distance of 50 mm from the distributor, while the upper port was placed 250 mm above the distributor, thus providing crucial information about the local bed dynamics. The pressure tap, flush with the column wall, was covered with a fine nylon mesh. The pressure transducers were carefully calibrated from volts to Pa using a pressure calibrator (Fluke Model 718). The calibration showed excellent linearity of voltage–Pa profiles.

Five hundred grams of the activated carbon was loaded in the bed before starting the experiment. The static height of the bed was 225 ± 3 mm. First, a number of fluidization and defluidization experiments were carried out using only nitrogen gas to study the fluidization hydrodynamics of the bed. There were initially some losses (<1% of the total solid mass) of the activated carbon due to elutriation, which were replenished to keep bed height constant throughout the experiment. These results, which are related to bed hydrodynamics, are reported elsewhere [47]. The adsorption experiments were carried out at a fixed velocity, while two different inlet CO_2 concentrations were considered as the composition of post combustion flue gases varies depending upon the fuel feedstock used for the power generation. As detailed later, the four different cases of particle mixing were carefully investigated. The opening, located at a distance of 500 mm above the distributor, was used as a port for monitoring the CO_2 concentration.

3. Results and Discussion

In this study, we considered four cases of particle mixing by varying the fraction of external Group B particles in the fluidized bed containing 500 g of activated carbon. In the first case, adsorption studies were carried out in the absence of the external particles. In the second case, 25 g Group B particles were added, and adsorption experiments were carried out. In the third case, the amount of external particles was increased to 50 g by further adding 25 g particles. In the fourth case, the total amount of external particles was 150 g; thus, the amount of external particles defined on the basis of the external particle free weight basis (X_1) were 0, 5, 10, and 30 wt %. All four cases will be individually discussed in this section before comparing the efficacy of the proposed strategy of particle mixing on the removal of CO_2 using the fluidized bed technology. We first present adsorbent characterization data, followed by the selection of the external particles for our proposed particle-mixing strategy. Next, we describe our experimental strategy before presenting the results of our investigation.

3.1. Adsorbent Characterization

We chose commercial reagent-grade activated carbon powder (Avonchem, Macclesfield, UK) as the adsorbent. The choice of activated carbons stemmed from extensive work reported in the literature, which have confirmed that despite their relatively low CO_2 adsorption capacity, activated carbons exhibit better stability, a very low sensitivity to moisture, and a large resistance to poisoning [48,49] and are therefore better suited for industrial applications. The adsorbent was characterized using surface area and porosity instrument (Micromeritics Tristar II, Norcross, GA, USA). Relevant characterization parameters are reported in Tables 1 and 2.

Table 1. Surface area (m^2/g) characterization of activated carbon.

Single point surface area at P/Po = 0.303993275:	953.84
BET Surface Area:	941.51
Langmuir Surface Area:	1437.38
t-Plot Micro-pore Area:	431.81
t-Plot External Surface Area:	509.70
BJH Adsorption cumulative surface area of pores 1.7–300.0 nm diameter	313.02
BJH Desorption cumulative surface area of pores 1.7–300.0 nm diameter	289.05

Table 2. Pore volume (cm^3/g) characterization of activated carbon.

t-Plot micropore volume	0.22973
BJH Adsorption cumulative volume of pores 1.7–300.0 nm diameter	0.29053
BJH Desorption cumulative volume of pores 1.7–300.0 nm diameter	0.28122

An important aspect of the adsorbent characteristics is its size distribution. Therefore, three runs were carried out using Malvern particle size analyzer to determine its size distribution. The average volume mean diameter was found to be 26.4 ± 1.1 μm [47]. The SEM micrograph of the sample is shown in Figure 2. Using experimental pressure drop versus superficial velocity data, the effective hydrodynamic diameter of the activated carbon was also evaluated with the help of the Ergun equation [47]. Its value was 27.5 μm, which is close to the size obtained from the particle size analysis. Such a close agreement between the two is a clear indication that there was almost no agglomeration of the adsorbent particles during the gas–solid contact in the bed. As part of a detailed investigation of the fluidization hydrodynamics, we also evaluated the fluidization index of the monocomponent bed of the activated carbon. Its value varied in the range of 0.76–0.80, indicating the presence of nonhomogeneities during fluidization [47]. Note that the bed nonhomogeneities always affect the effectiveness of the adsorbent particles present in the bed. In an ideal case, the fluidization index should be unity.
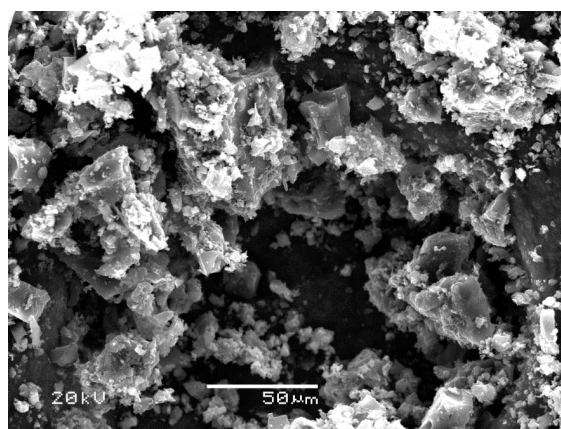

Figure 2. SEM images of adsorbent at a magnification of 500×.

3.2. Particle Mixing Scheme

The selection of external particles is crucial in the present particle-mixing strategy because the particle characteristics critically affect the fluidization hydrodynamics [22]. The group B particles used for mixing was inert sand of density 2664 kg/m^3. It was obtained by sieving the field sand in the lab and collecting the sample retained between 300 μm and 212 μm sieves, thus obtaining sample with a mean size of 256 μm. As shown in the Figure 3, addition of group B particles shifted the properties of the resulting mixture of adsorbent and external particles to group A, which generally yields particulate fluidization, thereby resulting in better mixing and higher mass transfer rates. Furthermore, inert nonporous external particles like sand does not pose any contamination risk.
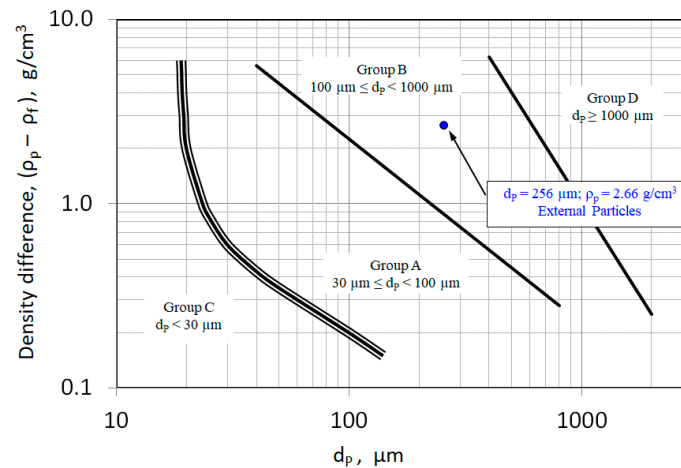

Figure 3. Geldart's classification-based particle-mixing strategy used for the proposed assisted fluidization technique.

For all four cases of particle mixing, the fluidization behavior was carefully investigated by monitoring the pressure drop versus velocity characteristics of the fluidized bed and evaluating the fluidization index [47]. It was obvious that particle mixing improved the fluidization hydrodynamics such that fluidization index as high as 0.95 was achieved with the addition of group B particles.

3.3. Experimental Strategy and Data Acquisition

The experimental setup was first tested for any leakage by ensuring the input and output gas flows were equal. Next, a three-step adsorption experiment was carried out. The first step was to start a controlled flow of nitrogen to test column containing the adsorbent for two hours (7200 s) to remove any traces of carbon dioxide and oxygen. During this purging step, the concentrations of both gases were monitored and recorded using the O_2/CO_2 analyzer. Next, the controlled flow of carbon dioxide was started for another two hours to allow its adsorption by the adsorbent present in the test section of the column. Finally, the CO_2 was stopped to let the desorption step proceed for another two hours before discontinuing the flow of nitrogen, as shown in Figure 4. The flow and duration of both nitrogen and CO_2 gas flows were always controlled using electronic mass flow controllers that were connected to the data acquisition system. By monitoring the gas concentration data, the duration of two hours (7200 s) was found to be sufficiently long to ensure completion of each of the three steps of the adsorption studies, i.e., purging, adsorption, and desorption. Thus, a total of six hours (21,600 s) were required for each complete adsorption experiment.
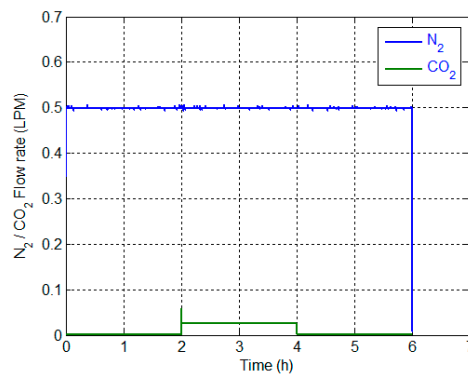
Figure 4. Flow rates of nitrogen and carbon dioxide during the experiment comprising consecutive purging, adsorption, and desorption steps.

The data sampling frequency was kept at 10 Hz, thus recording 10 data samples every second. Each data sample involved recording the following: (1) time, (2) pressure drop, (3) N_2 flow rate, (4) CO_2 flow rate, (5) CO_2 concentration, and (6) oxygen concentration. The O_2/CO_2 analyzer provided both CO_2 and O_2 concentrations. Note that all outputs were in volts and were converted into appropriate units with the help of calibration data. The responses of O_2/CO_2 analyzer are presented in Figure 5a,b, while the response of the CO_2 and N_2 mass flow controllers are shown in Figure 4. Note that the sharp decline in the oxygen concentration occurred (Figure 5b) due to purging of the experimental setup using nitrogen.
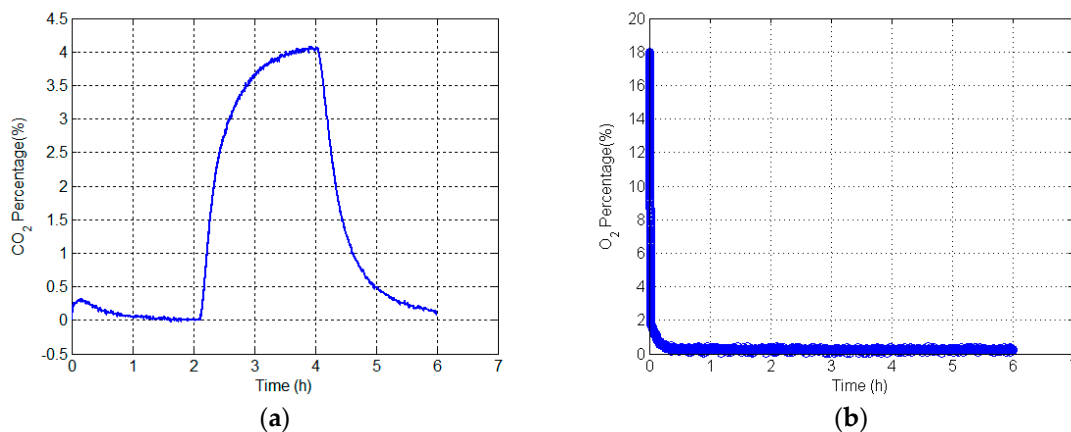

Figure 5. Response of O_2/CO_2 analyzer during the experiment comprising 2 h of purging, 2 h of adsorption, and 2 h of desorption steps over a total period of 6 h (**a**) CO_2 concentration; (**b**) O_2 concentration.

3.4. Experimental Results

First, we discuss the case of the CO_2 adsorption without the particles mixing, i.e., the fluidized bed containing only the activated carbon powder. Two different sets of experiments—Experiment 1 and Experiment 2—were carried out by keeping the inlet nitrogen flow fixed at 0.5 LPM and changing the CO_2 flow as shown in Figure 6. The concentration profiles are shown for both adsorption and desorption processes. During the adsorption, the CO_2 concentration asymptotically reached a constant value, which was expected as the bed of activated carbon gradually got saturated with the adsorbate. Similarly, a gradual decrease in the concentration was evident once the process of desorption was started by discontinuing the flow of the inlet CO_2 and leaving the nitrogen flow unchanged. The data recording in this particular experiment was stopped after 5000 s of desorption unlike other experiments where CO_2 concentration was monitored for 7200 s (2 h) as mentioned before. Note that 2 h purging

was always carried out to ensure removal of any remaining traces of the CO_2 in the fluidized bed before starting the process of adsorption.
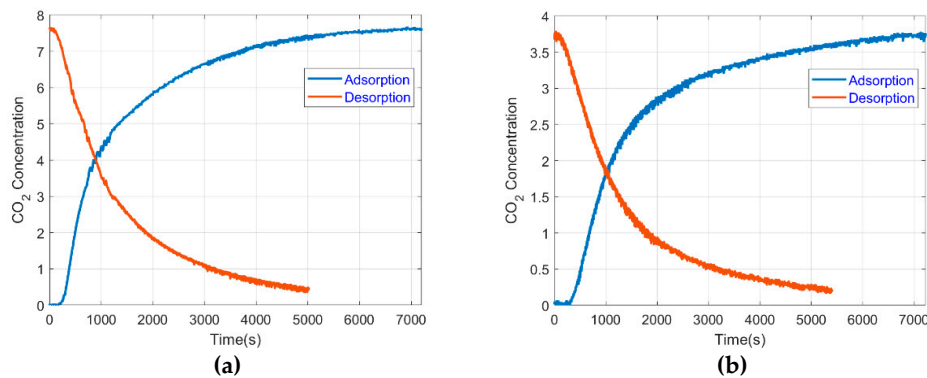

Figure 6. Variation in CO_2 concentration with time during the adsorption and desorption processes for the monocomponent fluidized bed of activated carbon (**a**) Experiment 1; (**b**) Experiment 2.

We have presented the experimental data in Figure 7, where the ordinate is the normalized CO_2 concentration obtained by dividing the instantaneous concentration by the inlet CO_2 concentration; the abscissa is time plotted on the logarithmic scale. Clearly, the CO_2 profile for Experiment 1 initially showed higher concentration compared to the one for Experiment 2. This can be attributed to faster saturation of the absorbent present in the fluidized bed due the higher CO_2 concentration in the inlet gas. In Figure 7b, the case of particle premixing is presented when small amount of external particle was added to the bed ($X_1 = 0.05$). Its breakthrough curves show similar trend observed for the monocomponent bed of activated carbon. The adsorption behavior of the bed for $X_1 = 0.10, 0.30$ is shown in Figure 7c,d, respectively, for both experiments.
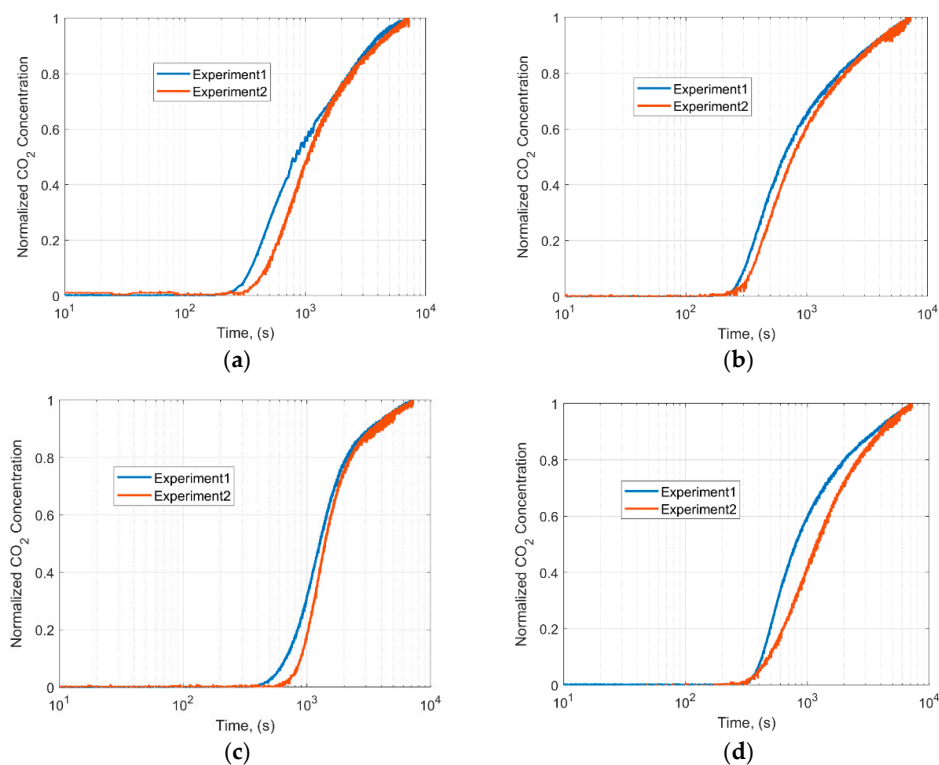

Figure 7. Response of the fluidized bed with particle mixing in different proportions of external group B particles (**a**) $X_1 = 0.00$; (**b**) $X_1 = 0.05$; (**c**) $X_1 = 0.10$; (**d**) $X_1 = 0.30$.

Our main objective was to examine the effect of particle mixing on the adsorption characteristics of the fluidized bed containing activated carbon. This is shown in Figure 8 for both high and low concentrations of the CO_2 in the inlet gas. Clearly, particle mixing made a significant difference on the CO_2 removal. As seen in Figure 8a, the addition of 25 g Group B particle surprisingly led to a concentration profile that exhibited higher CO_2 concentration than the monocomponent-activated carbon bed. This was a clear indication of lower CO_2 removal efficacy of the bed in this case. However, when the amount of external particles was increased to 50 g ($X_1 = 0.10$), the breakthrough curve showed a significant shift right, towards much lower CO_2 concentration compared to the previous two cases. Moreover, the time of breakthrough was also much higher. Increasing the fraction of particles to 150 g did not help as the breakthrough curve again shifted left, indicating lower CO_2 removal efficacy.
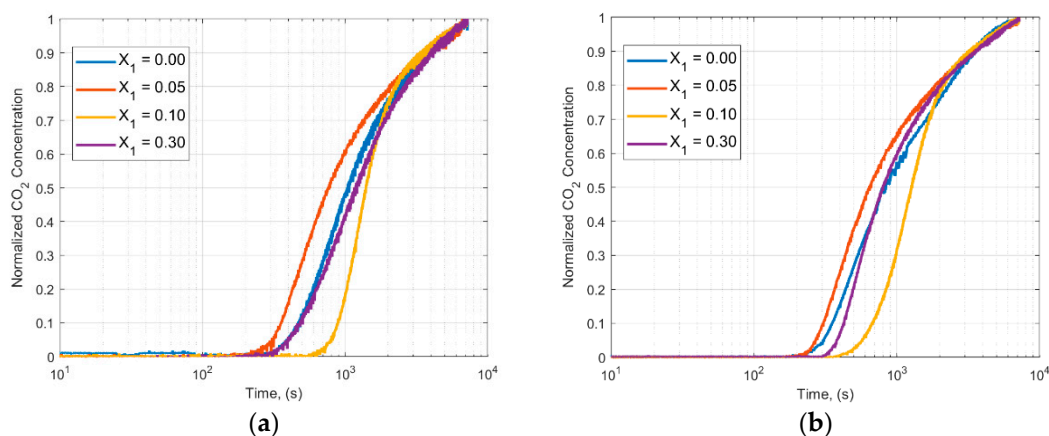

Figure 8. Effect of particle mixing on the response of the fluidized bed (**a**) Experiment 1; (**b**) Experiment 2.

Next, we consider the case of lower CO_2 concentration in the inlet gas (Figure 8b). Notwithstanding the change in the inlet concentration of CO_2, the breakthrough curves for different fractions of the external particles nonetheless showed the same trend. Adding 25 g sand decreased the CO_2 removal efficacy of the bed, while the best results were obtained with 50 g sand.

4. Conclusions

Results presented here clearly highlight the importance of the role of fluidization hydrodynamics. The addition of external particles improved the fluidization hydrodynamics, resulting in better quality of fluidization. This led to higher CO_2 removal efficiency of the fluidized bed. In this context, it is worthwhile to point out the results of our earlier investigation of the hydrodynamics of the same system comprising activated carbon and group B particles. A statistical analysis of the fluidization indices for different levels of particle mixing showed a similar trend. The hydrodynamics of mixed bed with 50 g group B particles was better than ones with 25 g and 150 g external particles. On the other hand, mixed fluidized bed of 25 g sand showed poor quality fluidization than its monocomponent counterpart [47]. We found the same effect of particle mixing in the present adsorption studies.

An important consideration in any assisted fluidization technique is the cost involved with its implementation and operation. Note that the main fluidization equipment did not require any modification or installation of any additional equipment for the implementation of the proposed technique of particle mixing. In addition, unlike other assisted fluidization techniques, there was no need for extra energy. The cost of the procurement of group B particles was almost negligible when using inert sand. Moreover, there was no contamination risk due to inert external particles. Combined together, these factors clearly highlight the potential of particle mixing as an effective strategy to improve the carbon dioxide capture efficacy of a fluidized bed containing fine adsorbent powder.

References

1. Trends in Global CO_2 and Total Greenhouse Gas Emissions: 2017 Report. Available online: http://www.pbl.nl/sites/default/files/cms/publicaties/pbl-2017-trends-in-global-co2-and-total-greenhouse-gas-emissons-2017-report_2674.pdf (accessed on 26 July 2018).

2. CO_2 Emissions by Countries. 2017. Available online: https://knoema.com/atlas/ranks/CO2-emissions?baseRegion=SA (accessed on 26 July 2018).

3. Lackner, K.; Gibbins, J.; Roddy, D.; Pocklington, D.; Logue, P.; Riley, N.; Chapman, S.J.; Nijnik, M.; Kitidis, V. *Issues in Environmental Science and Technology*; Hester, R.E., Harrison, R.M., Eds.; RCS Publishing: London, UK, 2009; pp. 1–308.

4. Creamer, A.E.; Gao, B. *Carbon Dioxide Capture: An Effective Way to Combat Global Warming*; Springer: Berlin, Germany, 2015; pp. 25–49. ISBN 978-3-319-17010-7.

5. CO_2 Capture Project, CCP Annual Report 2017. June 2018. Available online: http://www.co2captureproject.org (accessed on 26 July 2018).

6. MacDowell, N.; Florin, N.; Buchard, A.; Hallett, J.; Galindo, A.; Jackson, G.; Adjiman, C.; Williams, C.K.; Shah, N.; Fennel, P. An overview of CO_2 capture technologies. *Energy Environ. Sci.* **2010**, *3*, 1645–1669. [CrossRef]

7. Kargari, A.; Ravanchi, M.T. Carbon Dioxide: Capturing and Utilization, Greenhouse Gases-Capturing, Utilization and Reduction. ISBN 978-953-51-0192-5. Liu, G. InTech. 2012. Available online: http://www.intechopen.com/books/greenhouse-gases-capturing-utilization-and-reduction/carbon-dioxidecapturing-and-utilization/ (accessed on 26 July 2018).

8. Boundary Dam Carbon Capture Project. Available online: https://www.saskpower.com/our-power-future/infrastructure-projects/carbon-capture-and-storage/boundary-dam-carbon-capture-project (accessed on 13 August 2018).

9. Wang, Y.; Zhao, L.; Otto, A.; Robinius, M.; Stolten, D. A Review of Post-combustion CO_2 Capture Technologies from Coal-fired Power Plants. *Energy Procedia* **2017**, *4*, 650–665. [CrossRef]

10. Mushardt, H.; Müller, M.; Shishatskiy, S.; Wind, J.; Brinkmann, T. Detailed investigation of separation performance of a mmm for removal of higher hydrocarbons under varying operating conditions. *Membranes* **2016**, *6*, 16. [CrossRef] [PubMed]

11. Weigelt, F.; Georgopanos, P.; Shishatskiy, S.; Filiz, V.; Brinkmann, T.; Abetz, V. Development and characterization of defect-free matrimid® mixed-matrix membranes containing activated carbon particles for gas separation. *Polymers* **2018**, *10*, 51. [CrossRef]

12. Kassim, M.A.; Meng, T.K. Carbon dioxide (CO_2) biofixation by microalgae and its potential for biorefinery and biofuel production. *Sci. Total Environ.* **2017**, *584–585*, 1121–1129. [CrossRef] [PubMed]

13. Garcia, S.; Gil, M.V.; Martin, C.F.; Pis, J.J.; Rubiera, F.; Pevida, C. Breakthrough adsorption study of a commercial activated carbon for pre-combustion CO_2 capture. *Chem. Eng. J.* **2011**, *171*, 549–556. [CrossRef]

14. Valverde, J.M.; Pontiga, F.; Soria-Hoyo, C.; Quintanilla, M.A.S.; Moreno, H.; Duran, F.J.; Espin, M.J. Improving the gas solids contact efficiency in a fluidized bed of CO_2 adsorbent fine particles. *Chem. Phys.* **2011**, *13*, 14906–14909. [CrossRef] [PubMed]

15. Zukowski, W.; Englot, S.; Baron, J.; Kandefer, S.; Olek, M. Reduction of carbon dioxide emission using adsorption-desorption cycles in a fluidized bed reactor. *Environ. Prot. Eng.* **2010**, *36*, 47–56.

16. Gil, M.V.; Martinez, M.; Garcia, S.; Rubiera, F.; Pis, J.J.; Pevida, C. Response surface methodology as an efficient tool for optimizing carbon adsorbents for CO_2 capture, Fuel. *Process. Technol.* **2013**, *106*, 55–61. [CrossRef]

17. D'Alessandro, D.M.; Smit, B.; Long, J.R. Carbon dioxide capture: Prospects for new materials. *Angew. Chem. Int. Ed.* **2010**, *49*, 6058–6082. [CrossRef] [PubMed]

18. Plaza, M.G.; García, S.; Rubiera, F.; Pis, J.J.; Pevida, C. Post-combustion CO_2 capture with a commercial activated carbon: Comparison of different regeneration strategies. *Chem. Eng. J.* **2010**, *163*, 41–47. [CrossRef]

19. Ruiz, E.; Sánchez, J.M.; Maroño, M.; Otero, J. CO_2 capture from PCC power plants using solid sorbents: Bench scale study on synthetic gas. *Fuel* **2013**, *114*, 143–152. [CrossRef]

20. Abanades, J.C.; Anthony, E.J.; Lu, D.Y.; Salvador, C.; Alvarez, D. Capture of CO_2 from combustion gases in a fluidized bed of CaO. *AIChE J.* **2004**, *50*, 1614–1622. [CrossRef]

21. Valverde, M.; Duran, F.J.; Pontiga, F.; Moreno, H. CO_2 capture enhancement in a fluidized bed of a modified Geldart C powder. *Powder Technol.* **2012**, *224*, 247. [CrossRef]

22. Geldart, D. Types of Fluidization. *Powder Technol.* **1973**, *7*, 285–292. [CrossRef]

23. Ajbar, A.; Alhumaizi, K.; Asif, M. Improvement of the fluidizability of cohesive powders through mixing with small proportions of group a particles. *Can. J. Chem. Eng.* **2005**, *83*, 930–943. [CrossRef]

24. Zhu, C.; Liu, G.; Yu, Q.; Pfeffer, R.; Dave, R.; Nam, C. Sound assisted fluidization of nanoparticles agglomerates. *Powder Technol.* **2004**, *141*, 119–123. [CrossRef]

25. Ammendola, P.; Chirone, R.; Raganati, F. Fluidization of binary mixtures of nanoparticles under the effect of acoustic fields. *Adv. Powder Technol.* **2011**, *22*, 174–183. [CrossRef]

26. Ireland, E.; Pitt, K.; Smith, R. A review of pulsed flow fluidisation; the effects of intermittent gas flow on fluidised gas-solid bed behavior. *Powder Technol.* **2016**, *292*, 108–121. [CrossRef]

27. Ali, S.S.; Asif, M. Fluidization of nano-powders: Effect of flow pulsation. *Powder Technol.* **2012**, *225*, 86–92. [CrossRef]

28. Kaliyaperumal, S.; Barghi, S.; Zhu, J.; Briens, L.; Rohani, S. Effects of acoustic vibration on nano and sub-micron powders fluidization. *Powder Technol.* **2011**, *210*, 143–149. [CrossRef]

29. Valverde, J.M. Acoustic streaming in gas-fluidized beds of small particles. *Soft Matter* **2013**, *9*, 8792–8814. [CrossRef]

30. Ajbar, A.; Bakhbakhi, Y.; Ali, S.; Asif, M. Fluidization of nano-powders: Effect of sound vibration and pre-mixing with group A particles. *Powder Technol.* **2011**, *206*, 327–337. [CrossRef]

31. Ali, S.S.; Asif, M. Effect of particle mixing on the hydrodynamics of fluidized bed of nanoparticles. *Powder Technol.* **2017**, *310*, 234–240. [CrossRef]

32. Quintanilla, M.A.S.; Valverde, J.M.; Castellanos, A.; Lepek, D.; Pfeffer, R.; Dave, R.N. Nanofluidization as affected by vibration and electrostatic fields. *Chem. Eng. Sci.* **2008**, *63*, 5559–5569. [CrossRef]

33. Hristov, J. Magnetically assisted gas-solid fluidization in a tapered vessel: Part I. Magnetization-LAST mode. *Particuology* **2009**, *7*, 26–34. [CrossRef]

34. Ding, P.; Orwa, M.G.; Pacek, A.W. De-agglomeration of hydrophobic and hydrophilic silica nano-powders in a high shear mixer. *Powder Technol.* **2009**, *195*, 221–226. [CrossRef]

35. Bizhaem, K.H.; Tabrizi, H.B. Experimental study on hydrodynamic characteristics of gas-solid pulsed fluidized bed. *Powder Technol.* **2013**, *237*, 14–23. [CrossRef]

36. Ali, S.S.; Asif, M.; Ajbar, A. Bed collapse behavior of pulsed fluidized beds of nano-powder. *Adv. Powder Technol.* **2014**, *25*, 331–337. [CrossRef]

37. Akhavan, A.; Rahman, F.; Wang, S.; Rhodes, M. Enhanced fluidization of nanoparticles with gas phase pulsation assistance. *Powder Technol.* **2015**, *284*, 521–529. [CrossRef]

38. Ali, S.S.; Al-Ghurabi, E.H.; Ajbar, A.; Mohammed, Y.A.; Boumaza, M.; Asif, M. Effect of Frequency on Pulsed Fluidized Beds of Ultrafine Powders. *J. Nanomater.* **2016**, *4592501*, 1–12. [CrossRef]

39. Ammendola, P.; Chirone, R. Aeration and mixing behaviors of nano-sized powders under sound vibration. *Powder Technol.* **2010**, *201*, 49–56. [CrossRef]

40. Si, C.; Wu, J.; Wang, Y.; Zhang, Y.; Liu, G. Effect of acoustic field on minimum fluidization velocity and drying characteristics of lignite in a fluidized bed. *Fuel Process. Technol.* **2015**, *135*, 112–118. [CrossRef]

41. Raganati, F.; Ammendola, P.; Chirone, R. CO_2 capture by adsorption on fine activated carbon in a sound assisted fluidized bed. *Chem. Eng. Trans.* **2015**, *43*, 1033–1038.

42. Raganati, F.; Ammendola, P.; Chirone, R. CO_2 Adsorption on fine powders in a sound-assisted fluidized bed. In Proceedings of the XXXV Meeting of the Italian Section of the Combustion Institute, Milan, Italy, 10–12 October 2012; ISBN 978-88-88104-14-0.

43. Raganati, F.; Ammendola, P.; Chirone, R. CO_2 adsorption on fine activated carbon in a sound assisted fluidized bed: Effect of sound intensity and frequency, CO_2 partial pressure and fluidization velocity. *Appl. Energy* **2014**, *113*, 1269–1282. [CrossRef]

44. Raganati, F.; Gargiulo, V.; Ammendola, P.; Alfe, M.; Chirone, R. CO_2 capture performance of HKUST-1 in a sound assisted fluidized bed. *Chem. Eng. J.* **2014**, *239*, 75–86. [CrossRef]

45. Valverde, J.M.; Raganati, F.; Quintanilla, M.A.S.; Ebri, J.M.P.; Ammendola, P.; Chirone, R. Enhancement of CO_2 capture at Ca-looping conditions by high-intensity acoustic fields. *Appl. Energy* **2013**, *111*, 538–549. [CrossRef]

46. Ali, S.S.; Al-Ghurabi, E.H.; Ibrahim, A.A.; Asif, M. Effect of adding Geldart group A particles on the collapse of fluidized bed of hydrophilic nanoparticles. *Powder Technol.* **2018**, *330*, 50–57. [CrossRef]

47. Al-Ghurabi, E.H.; Ajbar, A.; Asif, M. Improving fluidization hydrodynamics of Group C particles by mixing with Group B particles. *Appl. Sci.* **2018**. under review.

48. Sjostrom, S.; Krutka, H. Evaluation of solid sorbents as a retrofit technology for CO_2 capture. *Fuel* **2010**, *89*, 1298–1306. [CrossRef]

49. Sjostrom, S.; Krutka, H.; Starns, T.; Campbell, T. Pilot test results of post combustion CO_2 capture using solid sorbents. *Energy Procedia* **2011**, *4*, 1584–1592. [CrossRef]